J. Fluid Mech. (1971), *vol.* 49, *part* 3, *pp.* 509–527
Printed in Great Britain

Selective withdrawal in rotating fluids

By HSING-HUA SHIH AND HSIEN-PING PAO

Department of Aerospace and Atmospheric Sciences,
The Catholic University of America, Washington, D.C.

(Received 26 January 1971)

An axisymmetric flow of a rotating fluid into a point sink was studied experimentally. The type of motion is mainly controlled by the value of the Rossby number R, a ratio of inertial and Coriolis forces. Experimental investigation shows that at a sufficiently large value of R the fluid motion resembles potential flow. However, as R falls below a critical number the withdrawal of the fluid starts to be selective. The flow field then divides into two regions; namely, a central flowing core and an almost stagnant region surrounding it.

It is observed that at a Rossby number below the critical value the flow field, induced by a sudden start of discharge at the sink, experiences several distinct stages during the course of each run. At the initial moment the flow exhibits a feature of potential flow. During the second stage, it develops into a state of selective withdrawal with an inviscid profile of a flowing core, which is the main interest of the present study. In the third stage, due to the unavoidable influence of the free or solid surface at the upstream, flow undergoes another change. The flowing core becomes a fast-spinning jet, in which the viscous force becomes important.

It is also found that once selective withdrawal begins, the angular velocity and flow rate of the flowing core differ substantially from the basic rotation and the actual discharge at the sink. During this second stage of flow development, the flowing core tends to adjust itself such that the intrinsic Rossby number $R'(= W_{\max}/2\Omega_c\delta_c)$ based on the properties of the flowing core, virtually remains constant for all values of R below the critical value. This constant value of R' is found to be about 0·36. The critical value of R which marks the beginning of the selective withdrawal is found to be in the neighbourhood of 0·26.

1. Introduction

The occurrence of velocity concentrations in various types of fluid systems is a well-known and interesting phenomenon. Selective withdrawal or the phenomenon of 'blocking' is one of the important features in a fluid system. The present work deals mainly with the selective withdrawal from rotating fluids.

Experimental observation shows that when a rotating fluid is removed at the bottom through a small hole, located at the axis of rotation of a tall cylindrical vessel, the type of motion is mainly controlled by the value of Rossby number. The Rossby number is defined as $R = Q/(2\pi\Omega b^3)$, in which Q is the flux, b is the radius of the vessel, and Ω is the angular velocity. At sufficiently large R the

motion differs little from the classical potential flow. As R decreases the sink draws more and more fluid from the central region along the axis of rotation, until at a certain critical R there appears a stagnant region surrounding a core of flowing fluid, which is the state of selective withdrawal.

Long's (1956) experiment first pointed out the existence of such a phenomenon of selective withdrawal. However, since the main interest of his experiment was other aspects of rotating fluids, no detailed measurements were done on selective withdrawal. In his paper Long gave a solution based on the steady axisymmetric inviscid equations of motion and uniform upstream condition. His solution describes the flow very well for Rossby number R greater than 0·261, above which no selective withdrawal appears. When R is in the neighbourhood of 0·261 there is an elongated eddy extending axially toward upstream, resulting in a return flow to infinity. The assumed upstream condition is hence violated and the flow pattern is also physically unstable, so that Long's theory does not describe the flow of selective withdrawal.

A very weak sink in a fast rotating flow field also leads to a velocity concentration. However, viscous effects become predominant. The problem was studied by Pao & Kao (1969). Their results show that the radius of the flowing core is independent of the sink strength.

It has been observed that many similarities exist between the flow of a rotating fluid and a stratified fluid. The problem of two-dimensional inviscid density-stratified fluid into a line sink was studied by Yih (1958), Trustrum (1964) and Kao (1965, 1970). Debler (1959) tested Yih's solution experimentally. The results of these studies indicate that selective withdrawal occurs for Froude number in the neighbourhood of above and below π^{-1}.

The main purpose of this paper is to determine the Rossby number characterizing the flow of selective withdrawal. Detailed velocity fields were investigated by methods of flow visualization, namely dye injection, PH indicator technique, and the hydrogen-bubble technique. The critical Rossby number for the selective withdrawal is derived from the data. The flow pattern and some other interesting features were studied. A theoretical investigation will be reported in part 2 of this paper.

2. Experimental apparatus and techniques

2.1. *The apparatus*

Basically, the system consisted of a rotating cylinder of fluid with a sink at the centre of its bottom. The details of this system are shown schematically in figure 1. The cylinder was made of Lucite and was 42 in. in length and had an inner diameter of 9·75 in. The cylinder was mounted on a horizontal turntable with its vertical axis coincident with the rotation axis of the turntable. Three levelling screws and four side-moving screws were installed on the turntable to provide minute adjustment for the correct alignment.

Fluid was extracted at the bottom through a hole of radius of $\frac{1}{8}$ in. The hole was connected to copper tubing passing through a steel hollow shaft. The shaft was mounted on two sets of thrust bearings, which were fixed to a massive angle-

iron frame. The frame was the main supporting structure for the whole apparatus. The copper tubing at the end of the hollow shaft was connected to a drainage pipe by means of a rotating seal. Fluid flowed through the pipe and then passed through a flowmeter to the outlet.

The turntable was driven with a uniform speed (usually between 0·1 and 0·8 rad/sec) by means of a $\frac{1}{4}$ h.p.d.c. motor through a V-belt system. The speed was

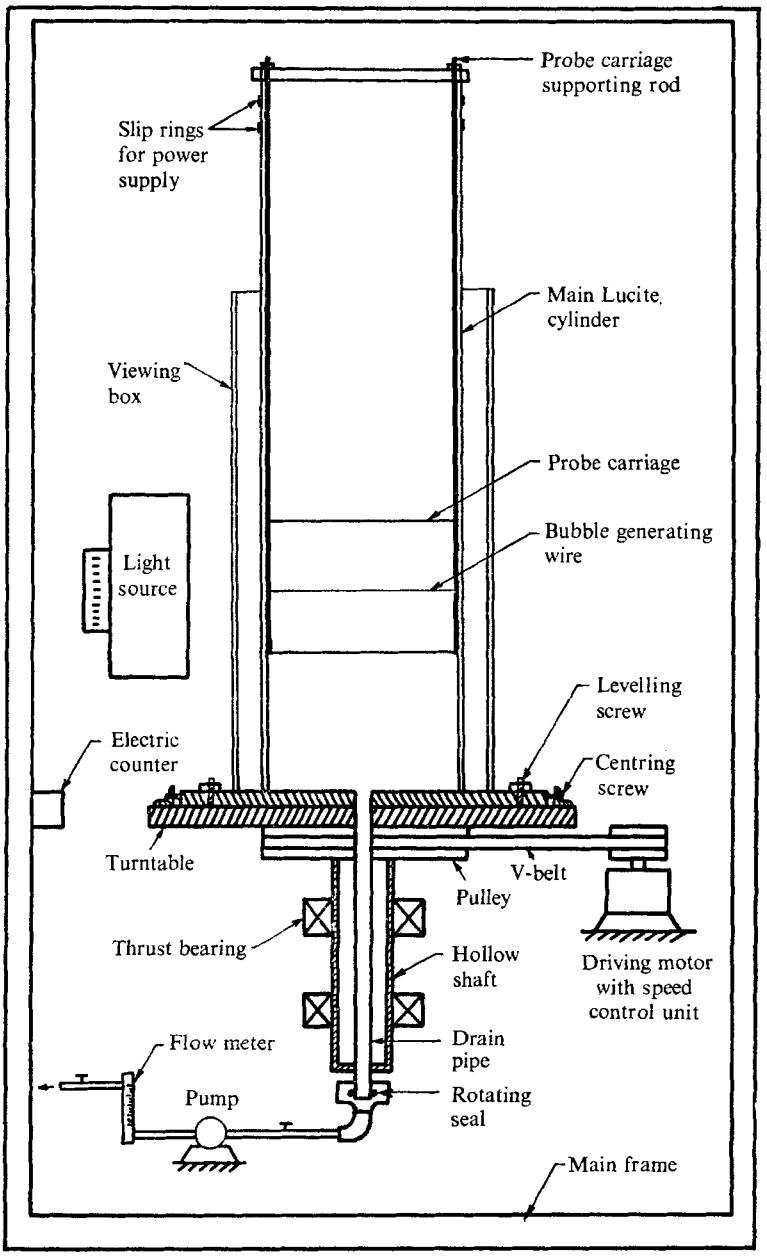

FIGURE 1. Apparatus layout (front view).

controlled through a silicon autotransformer unit. Constant rotation speed with variations less than 2 % during an average operation time of 2 h could be achieved.

A system of brass slip rings, fitted around the top end of the cylinder, served as contactors between the internal electrical system and the external power supply unit. Owing to the great difference in optical index between the air, the Lucite of the cylinder, and the water inside, there existed a serious optical distortion in the test section. To eliminate this distortion a rectangular box 3 ft high was constructed around the cylinder. The box was made of Lucite plates and was filled with clear water, forming an optical compensator.

2.2. *Methods of flow visualization*

Several methods of flow visualization were used for qualitative and quantitative measurements. The methods used here were dye injection, PH indicator and the hydrogen-bubble technique. The advantages of using these types of methods are that: disturbance to the flow is very small; multiple points measurement can be made at the same instant; it provides visual observation of the flow structure; a velocity profile can be obtained at one measurement; adequate accuracy is obtainable.

Dye injection gave a first crude picture of the overall flow pattern. Then the PH indicator and hydrogen-bubble techniques were used to obtain detailed information of the velocity field. The working fluid for the dye study and the PH indicator was Thymol Blue solution which is a PH indicator. The basic form is deep blue and the acidic form is light yellow. The solution can be used many times.

The PH indicator technique is good for measuring low velocities. The technique was described in detail by Baker (1966). A special advantage of this technique is that the coloured marker, which is essentially a fluid particle, is neutrally buoyant. However, for the present experiment it was observed that the higher axial velocity usually diluted the dye line very fast. The method was then used only for qualitative observations.

For quantative measurements we adopted the hydrogen-bubble technique. The technique utilizes the electrolysis of water to introduce hydrogen into the flow. A typical installation is to stretch a very fine wire across the region of flow which is to be studied. Electrical pulse is fed to the wire and the hydrogen formed is swept off the wire by the flowing water in the form of very small hydrogen bubbles. These bubbles can be made visible by a careful illumination.

The probe used for the hydrogen-bubble method consisted essentially of three fine wires stretched diametrically across a short piece of Lucite cylinder. A platinum and rhodium alloyed wire (0·002 in. diameter) was used. The Lucite cylinder was 6 in. long and 9·75 in. outside diameter, which was made to fit the inside dimension of the main cylindrical tank. The short cylinder, together with two supporting brass rods, constituted a probe carriage. The carriage could be moved up and down to any desired elevation. The two supporting rods also served to connect the electric current from the outside power supply to the electrodes of the probe. The hydrogen-bubble method has been described extensively in the literature (Davis & Fox 1967, Schraub *et al.* 1965), a detailed description is hence omitted here.

The photographic equipment included a Polaroid camera, a 35 mm framing Nikon camera with a remote control and motorized back attachment for single frame or continuous pictures.

3. General flow pattern

The general flow pattern was first studied under the condition that the upper surface of the fluid was always in contact with a solid surface which was fixed to the rotating cylinder. Later, the flow with the presence of a free upper surface emerged as a desirable condition, and its flow pattern was checked by dye injection.

In the case of a solid upper surface a closed circulating system was arranged, so that the fluid was kept under a constant head during the whole run. Fluid was first brought to a solid-body rotation, and then extracted from the bottom of the tank. Meanwhile, fluid was constantly replenished at the top through the distributed holes on the top plate. After the fluid had been running for about 30 min a small amount of dye was introduced with the feed-in fluid. The development of the dye pattern in time-elapsing sequence is shown in figure 2 (plate 1). Figure 2 (*a*) shows the convergence of flow through the Ekman boundary layer near the top plate. Some of the feed-in fluid was subsequently drawn into thin sheets wrapped around the axis of rotation in the later stage as shown in figure 2 (*c*). These thin sheets are essentially the so-called 'Taylor-walls' (Taylor 1921, Long 1954) which were engulfed by the flowing core along the axis of rotation. Outside the flowing core the vertical velocity component of the flow field was very small as indicated in figure 3, but the dye sheets kept on drifting downward very slowly. This relative motion between the dyed fluid and the basic flow field is mainly due to the unbalance of the pressure-gradient force and Coriolis force such that the rings of dyed fluid are compressed and forced to spread vertically.

It was observed that complex flow features existed in the flow field. They also changed as the physical parameters varied. Nevertheless, from these dye studies, certain general flow features that were common to the majority of cases studied could be drawn. As illustrated in figure 3, the flow field can be divided into several regions. The flowing portion of the fluid is mainly concentrated in region (I). It was observed that the angular velocity of this region was higher than that of the rest of the fluid. The increase of this angular velocity is believed to be due to the radial inflow induced during the initial period of the flow development. It is further increased in the later time due to the Ekman layer feed-in from the top region (VI). The wide annular zone (IV) is an almost stagnant region in which the fluid possesses only a very weak downward drifting velocity (usually about 3 % of the average axial velocity in region (I)). The angular velocity of this annular region was found to be slightly higher than the basic rotational speed of the tank. The top layer (VI) was found to have profound influence on the flowing core. The vertical layer (II) is a thin shear layer, resembling a cylindrical vortex sheet, in which the inertial force is probably more important than the Coriolis force. Locally the velocity profile must be modified by the viscous action. The vertical layer (V) along the side wall is rather weak. This is probably due to the fact that

the fluid in the annular region (IV) is almost motionless in the axial plane while the angular velocity there is only slightly higher than the basic rotation of the side wall. Thus the situation here is quite similar to the so-called 'Stewartson layers' (see Greenspan 1968) in which the inertial terms are unimportant.

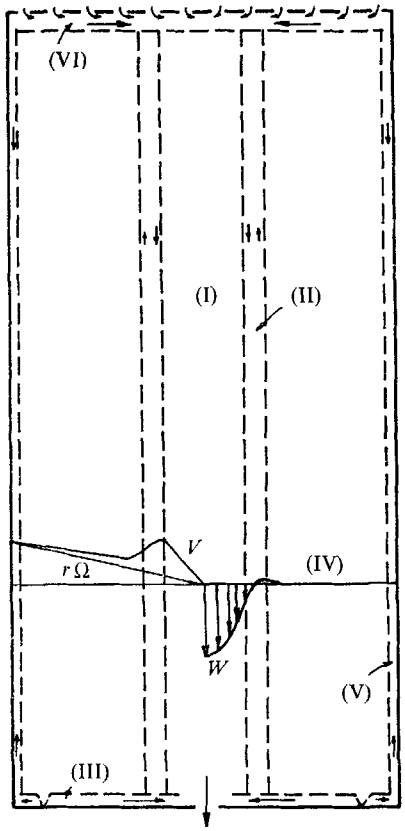

FIGURE 3. Sketch of the general flow structures in the presence of a solid upper boundary.

However, the phenomenon of blocking or selective withdrawal is inherently non-linear in nature, non-linear effects can be important even in the side-wall boundary layer.† Further investigation is needed in order to clarify this point. The bottom Ekman layer (III) is observed to be quite weak except in the region near the sink where the Ekman suction is enhanced by the fast-spinning motion of the flowing core.

In the free surface configuration, it was decided that no new fluid be supplied so as to minimize the possible disturbance at the upstream end. Detailed flow field measurements at various stages of flow development are given in the next section. The general flow pattern in the second stage of flow development with a

† Both referees pointed out that non-linear effects in side-wall boundary layers could be very important in some cases (see Lewellen 1965 and Hide 1968).

free upper boundary is shown in figure 4. Most features are similar to the previous case of a solid upper boundary, except that there is no apparent Ekman boundary layer near the free surface. However, it seems that a significant radial flow exists in this top region. The velocity profile in region (I) is essentially of the inviscid type and lasts until the end effects are felt.

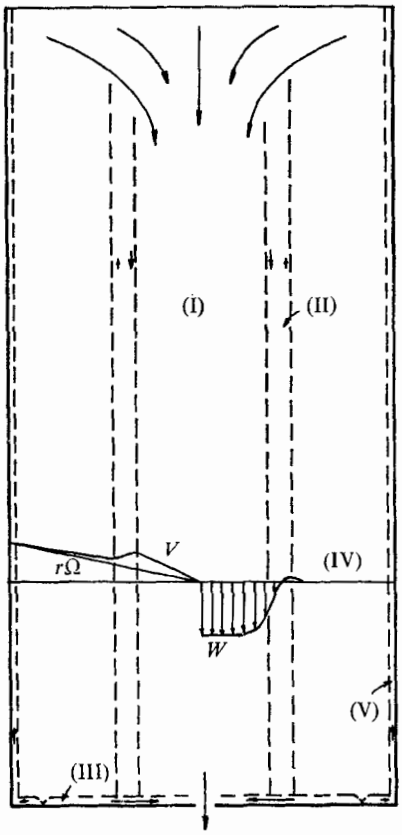

FIGURE 4. Sketch of the general flow structures in the second stage of flow development in the presence of a free upper boundary.

4. Flow field measurements

4.1. *Procedure*

Experiments concerning flow field measurements were conducted under the presence of a free upper surface without fluid replenishment. The sequence of events in running a typical test was as follows. Water was brought to a state of solid-body rotation after the main cylinder had rotated for about an hour. A rapid action valve was then opened and the pump was started. Water was extracted through the bottom hole of the tank and led to a flowmeter. The flow rate was recorded and was found to have little variation during the course of each run. Meanwhile, the flow pattern was observed constantly by pulsing the hydrogen-bubble generator. The information was recorded photographically by

a 35 mm framing camera. The test was completed in a time range from 40 sec to 15 min, depending on the flow rate and the rotating speed.

Two timers were used. One recorded the time lapse after the discharge started. The other, synchronizing the pulse generator, was used to record the travelling time of the hydrogen bubble and could be read to $\frac{1}{100}$ sec. The lighting equipment and the camera were both stationary.

The range of the rotation speed for the experiments was from 0·079 to 0·817 rad/sec. The value of discharge varied from 0·55 to 18·3 in.^{3}/sec. The corresponding Rossby numbers R covered were from 0·32 to 0·015. The axial velocities were measured at three axial positions (9 in., 13·5 in. and 21 in. above the sink). Tangential velocity profiles were measured at 9 in., 13·5 in., 21 in. and 27 in. above the sink. In all experiments the distance between the test section and the free surface was in the range 6 in. to 30 in.

Due to the limitation of the tank size, especially its axial length, it was difficult to achieve a completely steady state at the time of measurement. However, experimental results show that a quasi-steady state did exist in the present investigation, which will be discussed shortly.

Typical time-lapse photographs of the hydrogen bubbles in the axial plane are illustrated in figure 5 (plate 2). In evaluating the axial and tangential velocities, the image of the 35 mm film, superposed over the image of its corresponding length scale, was projected onto a screen. The projected image was about 1·5 times larger than the corresponding physical object. The velocities were determined by reading the bubble displacement and the corresponding elapsed time from each photograph. The core was subdivided into approximately ten radial positions for which axial velocities were determined. The core velocity profile was obtained by fitting the data points to a least-square best-fit curve.

The rising rate of the hydrogen bubble was calibrated in still water before each run. They varied from 0·1 in./sec to 0·2 in./sec. Since the value was relatively large, careful calibration and reasonable correction were necessary. The flow rate of the forward flowing core was then calculated from the plotted axial velocity profile for each test. The adjustment due to buoyancy effect was included.

4.2. *Flow development*

One of the difficult problems encountered in the experiments on rotating fluid flows is the time-dependent nature due to physical limitations of the laboratory set-up. Maxworthy (1968) reported the end effect of the container on the flow at low Rossby number in his experiment. Pritchard's (1969) experiment also indicated a strong unsteady nature.

In the present experiment it was observed that at a Rossby number R below the critical value the flow field, induced by a sudden start of a sink discharge, experiences several distinct stages of flow development during the course of each run (see figure 5). At the initial moment the flow resembles a potential flow in which no velocity concentration appears (figure 5(*a*)). Morgan's (1953) study on slow motions in rotating fluid also revealed the same finding on the appearance of the initial disturbed motion.

In the second stage, the flow develops into a selective withdrawal where the

flowing core possesses an inviscid axial velocity profile (figure 5(*b*)). A typical axial velocity obtained from the experimental data is shown in figure 6.

Due to the unavoidable influence of the end effect, resulting from the free or solid surface upstream, the flow subsequently changes into a fast-spinning jet. Viscosity becomes more and more important inside the jet. It should be noted that the second stage of the inviscid type would have persisted if upstream end effects were absent.

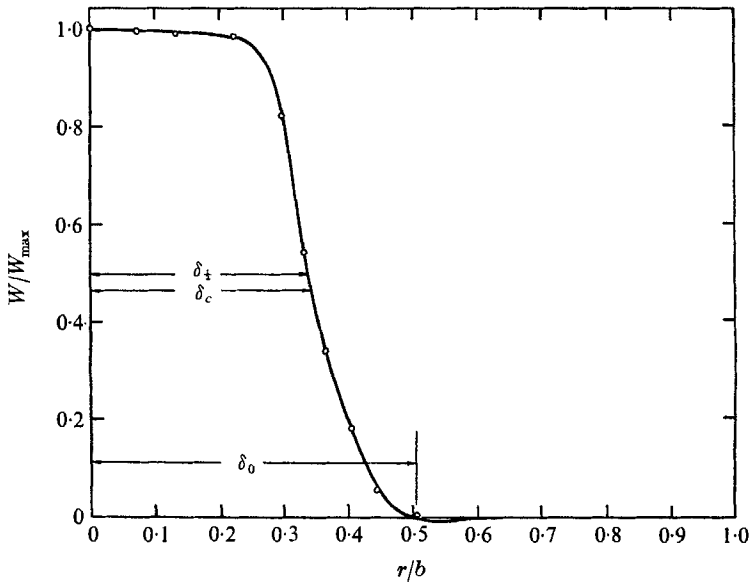

FIGURE 6. Typical axial velocity profile during the second stage of flow development.

The time development of the core radius, the maximum axial velocity and the angular velocity of the flowing core are plotted in figures 7, 8, and 9. The parameters in these plots are: the time scale $\Omega t/2\pi$ which is the period of the rotating tank after the sink has discharged for a time period of t; the dimensionless flowing core radius δ_0/b where δ_0 is the radius of the flowing core measured up to the point of zero axial velocity as shown in figure 6; the dimensionless axial centre velocity W_{max}/U where U is defined as $Q/\pi b^2$; and the ratio of the angular velocity of the flowing core and that of the tank Ω_c/Ω. The flatness in the central portion of these curves in figures 7, 8 and 9 indicates a very slow change in the flow pattern during the course of the time. Evidently, a quasi-steady state is indeed being reached during the second stage. The present work is mainly concerned with this stage of flow, since most geophysical flows away from boundaries are essentially inviscid in nature.

The typical tangential velocity profile during this stage is shown in figure 10. The time required to establish the second stage was about 5 sec to 50 sec corresponding to a range of Rossby number R from 0·015 to 0·32. During the second stage the inviscid axial velocity profile usually lasted about 30 sec to 4 min, depending on the basic rotating speed and the sink strength.

After this period of quasi-steady second stage, the flow then changed rapidly into a fast-spinning jet with a strong velocity concentration near the axis of rotation. Secondary flow circulation due to the presence of a free surface and the bottom end may contribute to this change.

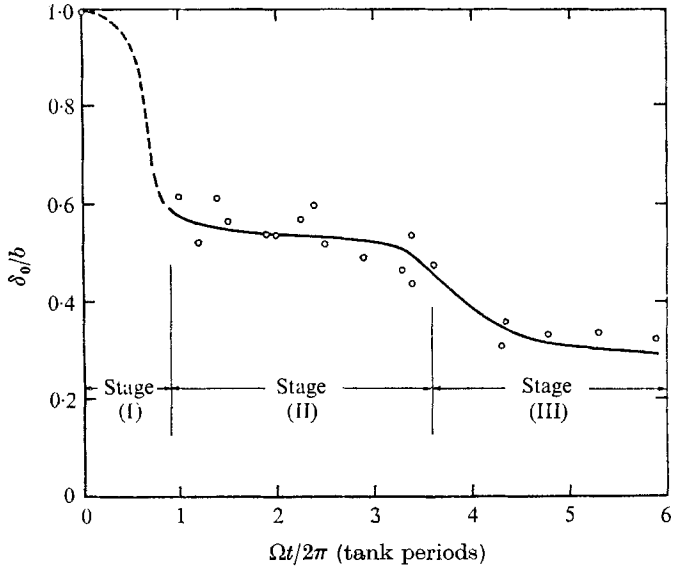

FIGURE 7. The development of the flowing core radius (R = 0·04).

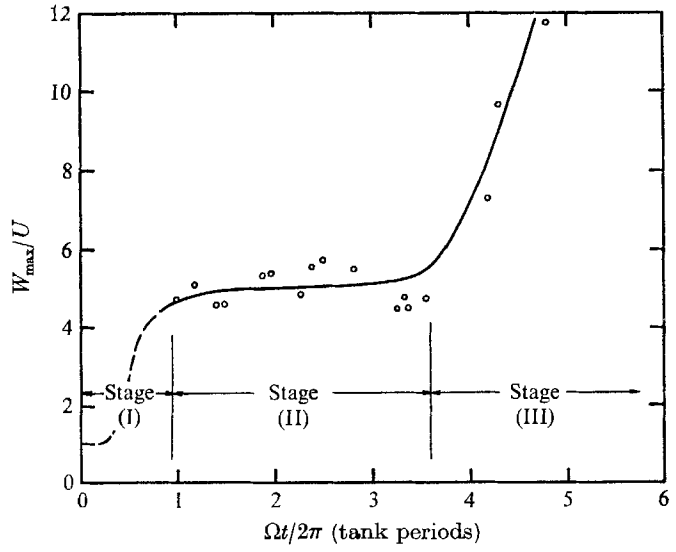

FIGURE 8. The development of the centre axial velocity of the flowing core (R = 0·04).

Information obtained from the tangential velocity profile is quite interesting. As shown in figure 10, the tangential velocity profile can be divided into three regions in general. In the central portion there is solid-body rotation with angular

velocity about twice as large as the basic rotating speed (see figure 11). This is due to the convergence of the angular momentum resulting from the radial inflow induced during the transition of the flow from the initial stage to the second

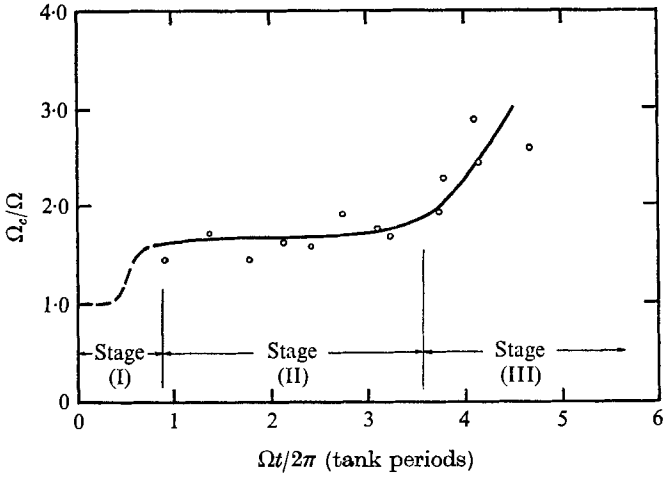

FIGURE 9. The development of the angular velocity of the flowing core (R = 0·039).

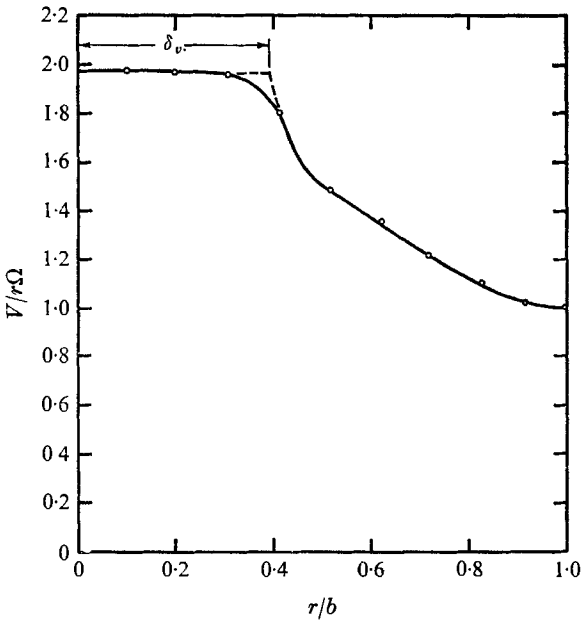

FIGURE 10. Typical angular velocity profile during the second stage of flow development (R = 0·054).

stage of selective withdrawal. This should not be surprising because similar situations indeed arise in the sink flow in the rotating fluid (Long 1956) just above the critical Rossby number and in the stratified fluid (Yih 1965) just above the critical Froude number. It is seen that the effective core size is shrinking and its

rotational speed (or density gradient in the case of stratified fluid) is increasing as the flow approaches the critical Rossby number. As a consequence, it is to be expected that the intrinsic Rossby number, based on the radius of the flowing core when selective withdrawal occurs, would be greater than 0·261 of Long's

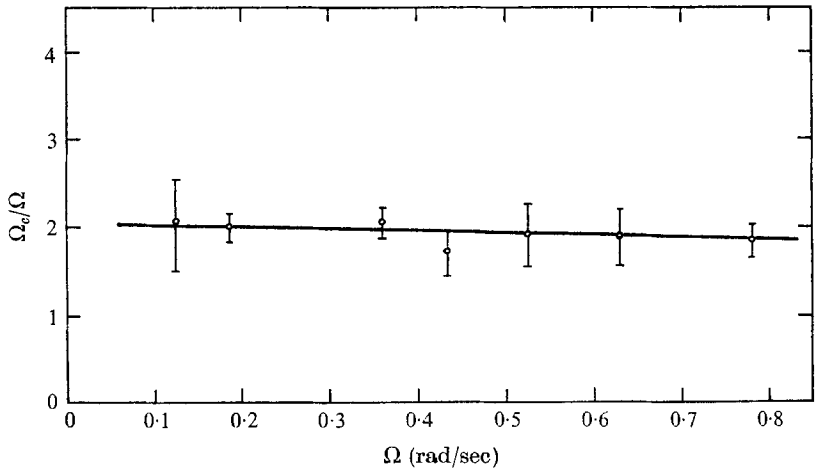

FIGURE 11. Comparison of the basic rotational speed with the angular velocity of the flowing core (at z = 9 in. above the sink).

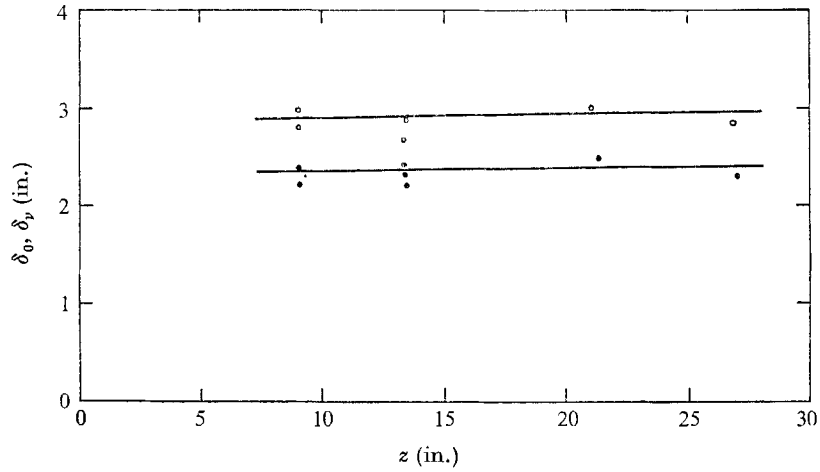

FIGURE 12. Comparison of core radius obtained from axial velocity profiles with that obtained from angular velocity profiles at various axial positions (R = 0·12). ○, from axial velocity profiles; ●, from angular velocity profiles.

(1956) critical value. In the outer region the angular velocity gradually decreases to the basic speed. Between these two regions there is a sharp transition in the angular velocity which coincides with the sharp transition in the vertical velocity as shown in figure 6.

Samples of the core sizes measured from axial and tangential velocity profiles are plotted in figure 12. It is seen that they are virtually independent of the axial distance z.

The relation between the flow rate Q measured by the flowmeter and the flow rate Q_c calculated from the forward velocity profile of the core is plotted in figure 13. It shows that except at very low discharge (below 2·0 in.^{3}/sec) the measured one is larger than the calculated one. This indicates that some fluid, other than that in the central flowing core, also flows into the sink. This added volume flux is probably supplied by the bottom Ekman boundary layer. It is

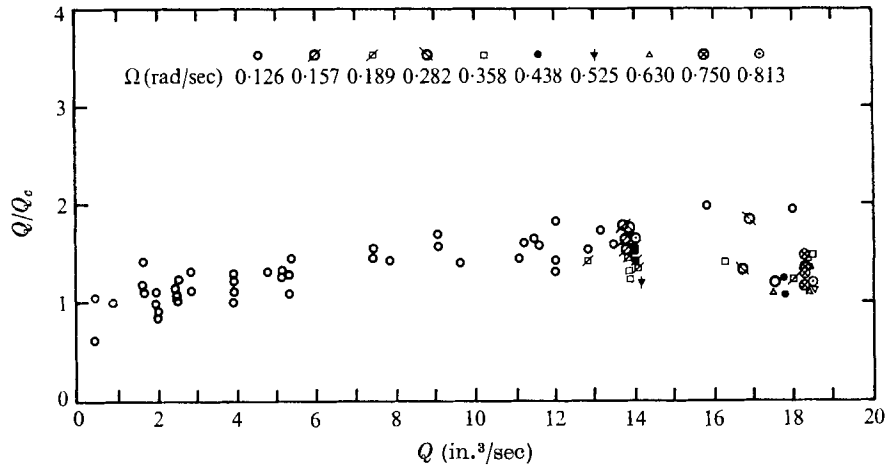

FIGURE 13. Comparison of measured discharge with the calculated forward flow rate of the central core.

interesting to note that the ratio Q/Q_c can be as large as two. This means that half of the flow discharge at the sink actually comes from the region other than the central flowing core. This Ekman layer suction is a unique situation in the rotating fluids (or vortex motion) which is absent in the stratified flows. Therefore, the word 'selective' must be read with caution here. We also note that, for a very low discharge, a substantial portion of the forward flowing core fluid returns to the main fluid as described in the viscous sink flow of Pao & Kao (1969).

5. Inviscid flowing core and intrinsic Rossby number

We now assume that the radius of the flowing core δ_0 is related to the following physical variables by

$$\delta_0 = f_1(z, Q, \Omega, \nu, t), \tag{1}$$

where z is the axial distance between the sink and the cross-section, Q is the volume flux through the sink, Ω is the angular velocity of the basic rotation, ν is the kinematic viscosity of the fluid, and t is the time lapsed since the sink started to discharge. Dimensional analysis then leads to the following dimensionless relation

$$\delta_0 \left(\frac{\Omega}{\nu z}\right)^{\frac{1}{3}} = f_2\left(\frac{Q}{\nu z}, \frac{Q\Omega^{\frac{1}{2}}}{\nu^{\frac{3}{2}}}, \frac{z}{t(\Omega\nu)^{\frac{1}{2}}}\right), \tag{2}$$

where $Q/\nu z$ is a Reynolds number, $Q\Omega^{\frac{1}{2}}/\nu^{\frac{3}{2}}$ is a Rossby number based on the

viscous core (defined as β by Pao & Kao (1969)), and $z/(\Omega\nu)^{\frac{1}{2}}$ is a time scale related to the secondary flow motion (Greenspan 1968).

A plot of $\delta_0(\Omega/\nu z)^{\frac{1}{3}}$ *vs.* $Q/(\nu z)$ is made as shown in figure 14. Some important consequences can be extracted from this graph. In this plot, the open circles are obtained from the flow field measurements during the second stage of flow

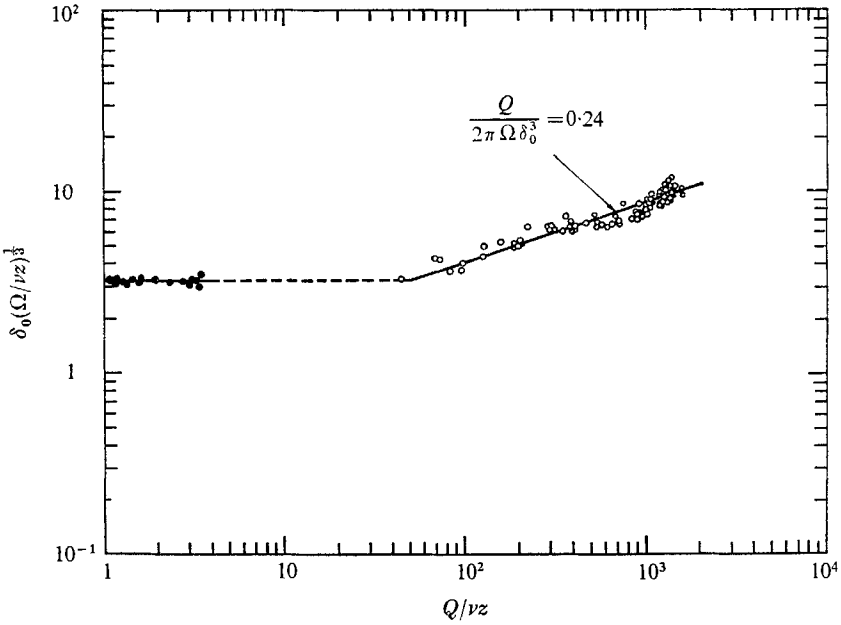

FIGURE 14. Core radius *vs.* Reynolds number. ●, viscous core data (Pao & Kao 1969); ○, present data.

development. They lie along regions of high Reynolds number where the viscous effect is seemingly negligible. A straight line with a slope of $\frac{1}{3}$ fits the data points quite well. This shows that the quantity $\delta_0(\Omega/\nu z)^{\frac{1}{3}}$ is virtually a function of $Q/\nu z$ only and, hence, is independent of the parameters $Q\Omega^{\frac{1}{2}}/\nu^{\frac{3}{2}}$ and $z/t(\Omega\nu)^{\frac{1}{2}}$. This also indirectly verifies that the second stage flow is indeed in a quasi-steady state. Moreover, the fact that the slope is $\frac{1}{3}$ is significant in that it shows that the viscous effect is indeed unimportant in that stage. This can be seen from the following derivation. Since the equation for this straight line is

$$\ln \delta_0(\Omega/\nu z)^{\frac{1}{3}} = \ln y_0 + \tfrac{1}{3}\ln (Q/\nu z), \tag{3}$$

where y_0 is the intercept on the $\ln (Q/\nu z) = 0$ line, it immediately leads to the relation

$$Q/2\pi\Omega\delta_0^3 = 1/2\pi y_0^3 = \text{constant} \tag{4}$$

which is an inviscid description for the selective withdrawal during the second stage of the flow development. The experimental result in figure 14 reveals that this constant value of the intrinsic Rossby number, defined as $R_1' = Q/(2\pi\Omega\delta_0^3)$, is about 0·24. The solid data points in the lower range of Reynolds number in figure 14 are taken from Pao & Kao's (1969) paper on viscous flowing core. That

result represents a different flow régime of selective withdrawal in which the Coriolis force is balanced by the viscous force, and the core radius becomes independent of the discharge Q. The theoretical relation for the viscous case is given by Pao & Kao

$$\delta_0(z) = 3{\cdot}245 z^{\frac{1}{3}}(\nu/\Omega)^{\frac{1}{3}}. \tag{5}$$

A transition region should exist between these two régimes.

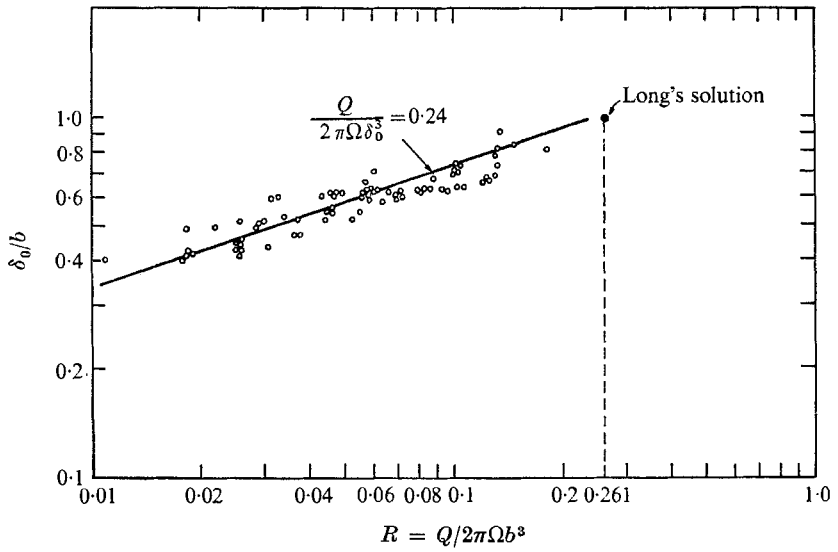

FIGURE 15. Core radius *vs.* Rossby number.

If we plot the same data in a graph of δ_0/b versus the Rossby number R as shown in figure 15, it is seen that R approaches a value near Long's critical number 0·261 as δ_0/b approaches one. A few experiments were conducted around this critical number. It was found that the critical Rossby number, for which the flow starts to separate, is in the neighbourhood of 0·24 to 0·28. Thus the whole picture becomes quite clear. For R greater than 0·261 Long's solution is capable of describing the flow. As R decreases to the neighbourhood of this value Long's solution yields an elongated eddy extending to upstream, which is physically unstable and the flow pattern must change. This indicates that blocking of the fluid must have occurred at a Rossby number near 0·261. The present experiment indeed shows that a flow of the type of selective withdrawal will take over approximately at $R = 0{\cdot}26$, although the dividing point for this transition is not a very clearcut one. Below this value, it is observed that the flowing core tends to adjust itself in such a way that the intrinsic Rossby number R_1' remains constant. The above observation seems to agree with the description given by Yih (1969) for blocking in a stratified fluid.

Since the rotational speed and forward flow rate of the flowing core are different from the basic rotational speed and discharge rate of the rotating vessel, it seems natural to introduce a new intrinsic Rossby number, R_2', based on the angular

velocity of the flowing core, Ω_c, and its flow rate Q_c. The adjusted results are shown in figure 16, in which the intrinsic Rossby number, defined as $R_2' = Q_c/(2\pi\Omega_c\delta_0^3)$, becomes about 0·10.

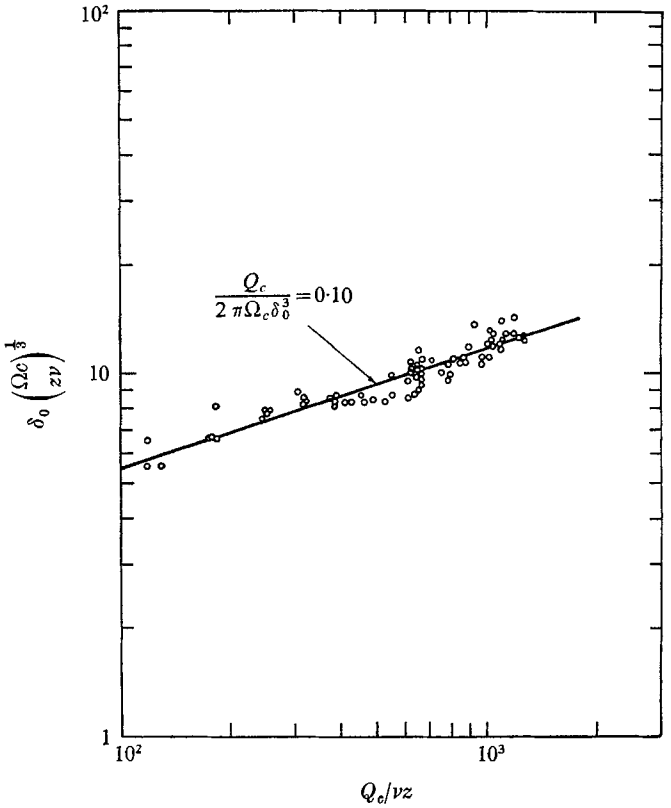

FIGURE 16. Core radius *vs.* Reynolds number (modified).

It should be noted, however, that the flowing radius δ_0, used in the data presentations, was measured to the point where the forward flowing axial velocity falls to zero, as shown in figure 6. Therefore, caution must be exercised before any comparison with the analytical inviscid solution is made. In order to compare with the inviscid solution to be presented in a subsequent paper, an adjustment for the thickness of the viscous layer around the flowing core is necessary. Theoretically, the radius of the inviscid core should be defined as

$$\delta_c = (Q_c/\pi W_{\max})^{\frac{1}{2}}. \tag{6}$$

In other words, the equivalent size of the inviscid core is defined as the radius of a uniform core flow with the same volume flow rate. With the radius of the inviscid core δ_c replacing δ_0, a plot similar to figure 14 is now shown in figure 17. Again, a straight line with a slope of $\frac{1}{3}$ fits the data quite well. This immediately leads to the relation

$$R' \equiv \frac{Q_c}{2\pi\Omega_c\delta_c^3} \equiv \frac{W_{\max}}{2\Omega_c\delta_c} = 0{\cdot}36. \tag{7}$$

The fact that the intrinsic Rossby number of the inviscid core R' is larger than the critical Rossby number 0·26 is to be expected since the effective core size and its rotational speed experience a drastic change as the flow approaches the critical Rossby number.

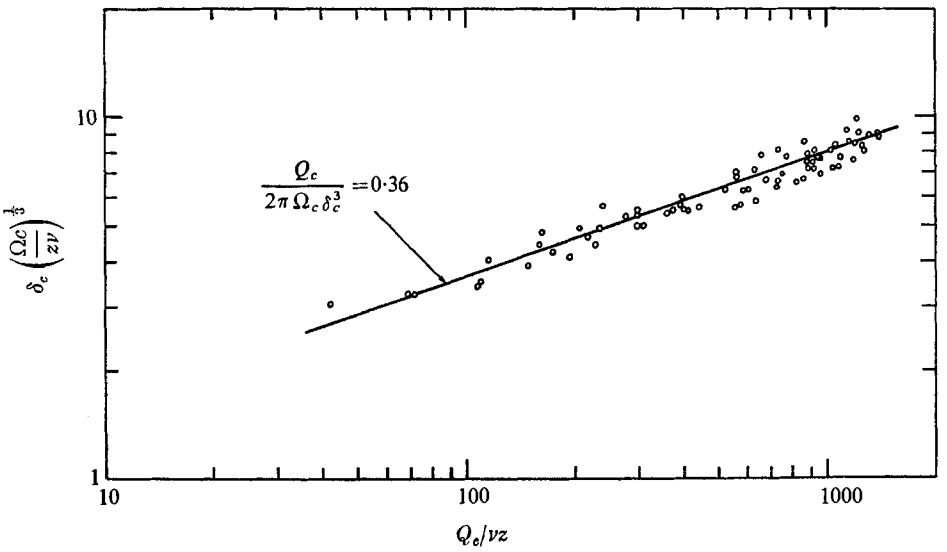

FIGURE 17. Core radius *vs.* Reynolds number based on δ_c, Q_c and Ω_c.

It should be noted that δ_c as defined above is only slightly larger than $\delta_{\frac{1}{2}}$ as shown in figure 6, where $\delta_{\frac{1}{2}}$ is the value of the radius at which the axial velocity is one half of the maximum axial velocity $W_{\max}$. In fact, the difference between δ_c and $\delta_{\frac{1}{2}}$ is so small that $\delta_{\frac{1}{2}}$ may substitute for δ_c in all practical applications.

Finally, a word about the experiment of Debler (1959) which is the counterpart of the present one, in the density-stratified fluid. His experiments showed that the intrinsic Froude number F' remained approximately constant for all separated flows with an average $F' = 0{\cdot}26$. This value is believed to be the counterpart of the present $R_1' = 0{\cdot}24$ for rotating flows. Since no detailed measurements on the velocity profiles were made by Debler, the equivalent inviscid depth of the discharging layer cannot be calculated accurately. An intelligent guess, based on the present experiment in rotating fluids, would put the intrinsic Froude number F' of all separated flows in the range 0·35–0·40 where F' is based on the inviscid depth and density gradient of the discharging layer.

6. Conclusions

Experimental investigation was made of the effect of a hydrodynamic sink at the axis of rotation of a tall cylinder. The phenomenon of selective withdrawal was carefully studied. From the present study, we draw the following conclusions:

(i) Experiment shows that selective withdrawal occurs for all flows with the

Rossby number R less than a critical value which is about 0·26, provided the end effect is absent. Above this value the flow pattern resembles that of potential flow, for which Long's solution is valid. Below this critical number the flow is characterized by the presence of a central flowing core and an almost stagnant region surrounding it. The radius of the flowing core tends to adjust itself such that the intrinsic Rossby number R' based on the properties of the flowing core, remains constant. The value of the constant depends on the definition of the core radius. Corresponding to an equivalent inviscid core, the value of the intrinsic Rossby number is found to be about 0·36.

(ii) It is observed that at a Rossby number R below the critical value the flow field, induced by a sudden start of discharge at the sink, experiences several distinct stages during the course of each run. At the initial instant the profile exhibits a potential flow pattern. It then develops into an almost inviscid velocity profile which resembles the inviscid core flow to be discussed in a subsequent paper. As the free surface draws down further, end effects will be felt, the flowing core changes into a fast-spinning narrow jet in which the viscous effect then becomes increasingly important.

The first stage is of a transient nature, while the second stage behaves very much like a steady state. The third stage is dominated by the upstream end effect; in the case of free surface, this stage is unsteady. The present work is concerned mainly with flow in the second stage, which is believed to be of some geophysical significance.

(iii) The measured discharge is usually larger than the calculated flow rate carried by the forward flowing core. This indicates that the bottom Ekman layer has evidently brought in the additional fluid to the sink.

(iv) The central core usually possesses a higher angular velocity which is on the average about twice as fast as the basic rotation.

This work was supported by the Atmospheric Sciences Section, National Science Foundation, NSF Grants GA-10825 and GA-23784.

REFERENCES

Baker, D. J. 1966 *J. Fluid Mech.* **26**, 573.
Davis, W. & Fox, R. W. 1967 *J. Basic Engrg. ASME* Paper no. 66-WA/FE-21, 771.
Debler, W. R. 1959 *Proc. Am. Soc. Civil Engrs.* **85**, 51.
Greenspan, H. P. 1968 *The Theory of Rotating Fluids.* Cambridge University Press.
Hide, R. 1968 *J. Fluid Mech.* **32**, 737.
Kao, T. W. 1965 *J. Fluid Mech.* **21**, 535.
Kao, T. W. 1970 *Phys. Fluids*, **13**, 558.
Lewellen, W. S. 1965 *A.I.A.A. J.* **3**, 91.
Long, R. R. 1954 *J. Met.* **11**, 247.
Long, R. R. 1956 *Quart. J. Mech. Appl. Math.* **9**, 358.
Maxworthy, T. 1968 *J. Fluid Mech.* **31**, 643.
Morgan, G. W. 1953 *Proc. Cam. Phil. Soc.* **49**, 362.
Pao, H. P. & Kao, T. W. 1969 *Phys. Fluids*, **12**, 1536.
Pritchard, W. G. 1969 *J. Fluid Mech.* **39**, 443.

SCHRAUB, F. A., KLINE, S. J., HENRY, J., RUNSTADLER, J. W. & LITTELL, A. 1965 *J. Basic Engrg ASME* Paper no. 64-WA/FE-20.

TAYLOR, G. I. 1921 *Proc. Roy. Soc.* A **100**, 114.

TRUSTRUM, K. 1964 *J. Fluid Mech.* **19**, 415.

YIH, C. S. 1958 *Proc. 3rd U.S. Nat. Cong. Appl. Mech.* 857.

YIH, C. S. 1965 *Dynamics of Non-Homogeneous Fluids.* New York: Macmillan.

YIH, C. S. 1969 *Annual Review of Fluid Mech.* **1**, 98.

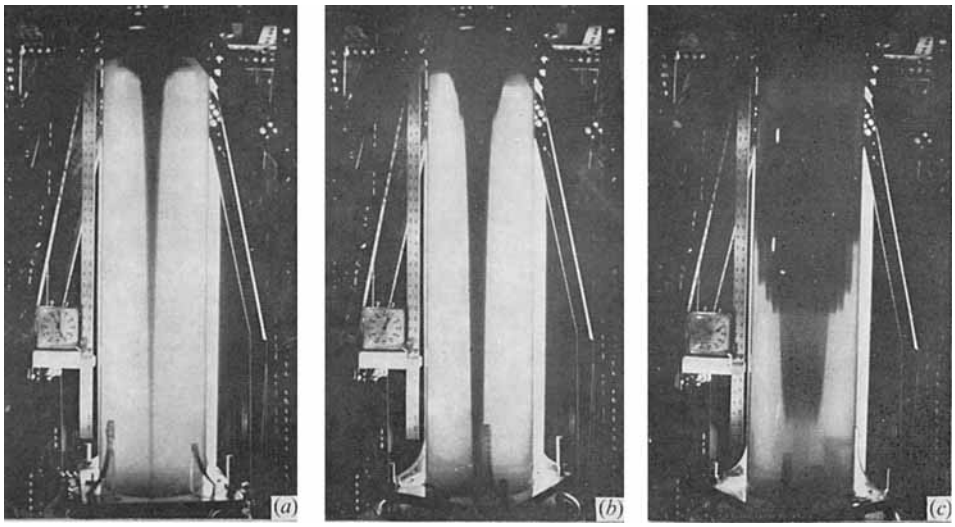

FIGURE 2. Development of the dye pattern in the presence of a solid upper boundary. The experimental conditions are: $\Omega = 15$ rev/min, $Q = 1{\cdot}714$ in.^{3}/sec. A small amount of dye was introduced after the fluid had been running for about 30 min. The pictures show the dye pattern in time-elapsing sequence: (*a*) 55 sec; (*b*) 8 min 27 sec; (*c*) 33 min 42 sec.

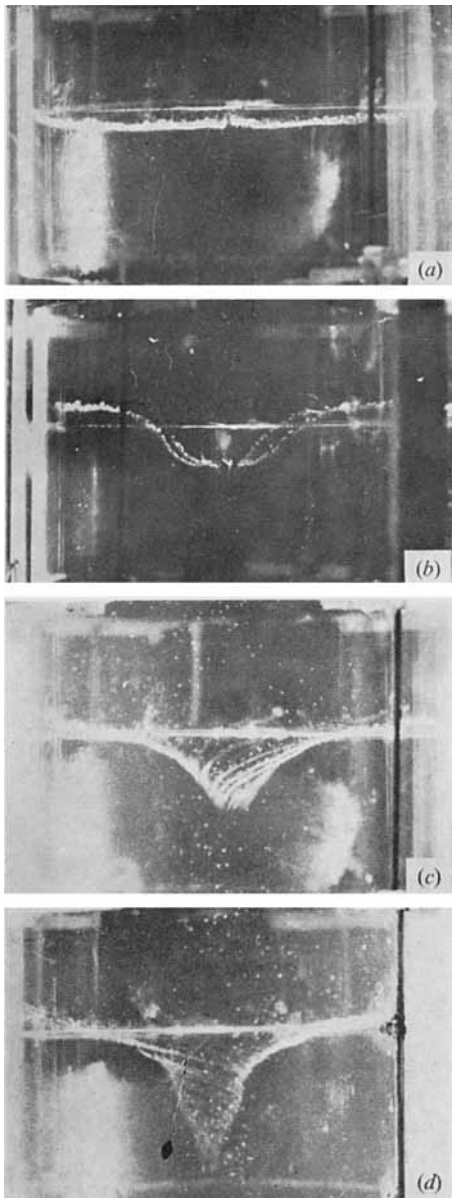

FIGURE 5. Stages of flow development. The experimental conditions are: $\Omega = 1{\cdot}12$ rev/min, $Q = 3{\cdot}918$ in.^{3}/sec. Hydrogen bubbles show the axial velocity profiles in time sequence after the opening of the sink valve: (*a*) Initial stage 2·8 sec; (*b*) 2nd stage 173·0 sec; (*c*) 3rd stage 252·0 sec; (*d*) 3rd stage 290·0 sec.